Helicity scalings

2011 J. Phys.: Conf. Ser. 318 042013

(http://iopscience.iop.org/1742-6596/318/4/042013)

Journal of Physics: Conference Series **318** (2011) 042013 doi:10.1088/1742-6596/318/4/042013

Helicity scalings

F. Plunian[1], T. Lessinnes[2], D. Carati[2], R. Stepanov[3]

[1]ISTerre, CNRS, Université Joseph Fourier, Grenoble, France,
[2]Physique Statistique et Plasmas, Université Libre de Bruxelles, Belgium
[3]Institute of Continuous Media Mechanics of the Russian Academy of Science, Perm, Russia

E-mail: Franck.Plunian@ujf-grenoble.fr

Abstract. Using a helical shell model of turbulence, Chen *et al.* (2003) showed that both helicity and energy dissipate at the Kolmogorov scale, independently from any helicity input. This is in contradiction with a previous paper by Ditlevsen & Giuliani (2001) in which, using a GOY shell model of turbulence, they found that helicity dissipates at a scale larger than the Kolmogorov scale, and does depend on the helicity input. In a recent paper by Lessinnes *et al.* (2011), we showed that this discrepancy is due to the fact that in the GOY shell model only one helical mode (+ or −) is present at each scale instead of both modes in the helical shell model. Then, using the GOY model, the near cancellation of the helicity flux between the + and − modes cannot occur at small scales, as it should be in true turbulence. We review the main results with a focus on the numerical procedure needed to obtain accurate statistics.

1. Introduction

Helicity is a scalar quantity which, like energy, is quadratically invariant. It means that the flux of helicity is constant along a range of scales between the forcing (large) scale of motion and the scale k_H^{-1} below which helicity dissipates. Using a GOY shell model of turbulence Ditlevsen & Giuliani (2001) suggested that $k_H^{-1} > k_E^{-1}$, where k_E^{-1} is the scale of energy dissipation. They expect two inertial ranges, one with coexisting cascades of energy and helicity at scales larger than k_H^{-1}, and a range between k_H^{-1} and k_E^{-1} where the flow is non helical.

In contrast, using an other shell model of turbulence based on helical wave decomposition, Chen *et al.* (2003) found that both scales were equal $k_H^{-1} = k_E^{-1}$, implying that the idea of two inertial ranges is irrelevant. They confirmed their results with direct numerical simulation though, as noted by the authors, the computational limitations prevent them to have a Reynolds number sufficiently large to really discriminate between both scenarii.

In Lessinnes *et al.* (2011), we explain why such a discrepancy occurs between both shell models, GOY and helical. Decomposing the velocity into positively and negatively polarized helical waves (±), we show that the scale k_H^{-1} found in the GOY model is in fact $k_{H^\pm}^{-1}$, the scale of helicity dissipation for each helical wave. As found by Ditlevsen & Giuliani (2001) we may have $k_{H^\pm} < k_E$. However we always have $k_H = k_E$ as found by Chen *et al.* (2003).

2. Kolmogorov phenomenology

Before going into the details of the two shell models we come back on the Kolmogorov scaling analysis. From now we assume isotropy, considering that the spectral quantities E and H depend

on $k = |\mathbf{k}|$. In the inertial range the non linear transfer rates of energy and helicity must satisfy

$$\varepsilon \sim kE(k)/\tau_E(k), \qquad \delta \sim kH(k)/\tau_H(k) \tag{1}$$

where ε and δ are respectively the injection rate of energy and helicity, $\tau_E(k)$ and $\tau_H(k)$ characteristic times of transfer. Assuming that both times are equal to the turn over time

$$\tau_E(k) \sim \tau_H(k) \sim k^{-1}u(k)^{-1} \tag{2}$$

with

$$u(k) \sim k^{1/2}E(k)^{1/2}, \tag{3}$$

leads to

$$E(k) = C_E\varepsilon^{2/3}k^{-5/3}, \qquad H(k) = C_H(\delta/\varepsilon^{1/3})k^{-5/3} \tag{4}$$

where C_E and C_H are some constants. As noted in Ditlevsen & Giuliani (2001), taking $u(k) \sim H(k)^{1/2}$ instead of (3) and replacing it in (2) would be misleading unless no energy is injected in the system, that we do not consider here.

Following the line of developments by Ditlevsen & Giuliani (2001), the velocity in the spectral space can be expanded in a basis of polarized helical waves $\mathbf{h}^\pm$ defined by $i\mathbf{k} \times \mathbf{h}^\pm = \pm k\mathbf{h}^\pm$ (see for example Waleffe (1992)). Using incompressibility $\mathbf{k} \cdot \mathbf{u}(\mathbf{k}) = 0$ we have $\mathbf{u}(\mathbf{k}) = u^+(\mathbf{k})\mathbf{h}^+ + u^-(\mathbf{k})\mathbf{h}^-$. The energy and helicity in the mode $\mathbf{u}(\mathbf{k})$ then become respectively

$$\mathbf{u}(\mathbf{k}) \cdot \mathbf{u}^*(\mathbf{k})/2 = (|u^+(\mathbf{k})|^2 + |u^-(\mathbf{k})|^2)/2 \tag{5}$$
$$\mathbf{u}(\mathbf{k}) \cdot \omega^*(\mathbf{k})/2 = k(|u^+(\mathbf{k})|^2 - |u^-(\mathbf{k})|^2)/2 \tag{6}$$

where $\omega(\mathbf{k})$ is the vorticity in the spectral space.

Introducing the spectral densities of energy and helicity for the helical modes $\pm$, we have

$$E(k) = E^+(k) + E^-(k) \tag{7}$$
$$H(k) = H^+(k) + H^-(k) \tag{8}$$
$$H^\pm(k) = \pm kE^\pm(k). \tag{9}$$

Then, from (4) we have

$$E^+(k) = (C_E/2)\varepsilon^{2/3}k^{-5/3} + (C_H/2)(\delta/\varepsilon^{1/3})k^{-8/3} \tag{10}$$
$$E^-(k) = (C_E/2)\varepsilon^{2/3}k^{-5/3} - (C_H/2)(\delta/\varepsilon^{1/3})k^{-8/3} \tag{11}$$

which are the equations (9) and (10) of Ditlevsen & Giuliani (2001). Then in addition to (4), in the inertial range we expect at leading order in k

$$E^\pm(k) = \frac{C_E}{2}\varepsilon^{2/3}k^{-5/3}, \; H^\pm(k) = \pm\frac{C_E}{2}\varepsilon^{2/3}k^{-2/3}. \tag{12}$$

From the Navier-Stokes equation in the spectral space, we can show that the quantity X, standing for E or H must satisfy the equation

$$\partial_t X^s(k,t) = T^s_X(k,t) - 2\nu k^2 X^s(k,t) + F^s_X(k,t) \tag{13}$$

where the superscript s is used only when dealing with helical modes. The quantities T^s_X and F^s_X are the non linear transfer function and injection rate of X, in the helical mode s ($= \pm$) or

in both modes (without superscript). The time rate of change of X^s due to the non linear terms in (13) is defined by

$$\Pi_X^{s<}(k,t) = -\int_0^k T_X^s(p,t)dp. \tag{14}$$

For $s = \pm$, it defines the flux of X from scales smaller than k in the helical mode s, towards all scales of the other helical mode $-s$, and towards scales larger than k in the same helical mode s. A crucial difference between the flux from both modes $\Pi_X^<$ and the ones from each mode $\Pi_X^{\pm<}$ is that the latter also includes the flux at the same scale from one mode to the other. Assuming a stationary statistical state, its time average satisfy

$$\Pi_X^{s<}(k) = F_X^s - 2\nu\int_0^k p^2 X^s(p)dp \tag{15}$$

where the injection rates are denoted $F_E = \varepsilon$, $F_H = \delta$, $F_E^\pm = \varepsilon^\pm$, $F_H^\pm = \delta^\pm$ (with $\delta^- < 0$). Assuming that they occur at the same scale k_F, they satisfy $\varepsilon = \varepsilon^+ + \varepsilon^-$ and $\delta = \delta^+ + \delta^- = k_F(\varepsilon^+ - \varepsilon^-)$.

Replacing (4) and (12) in (15) we find the following fluxes in the inertial range

$$\Pi_E^< = \varepsilon - \frac{3}{2}C_E\nu\varepsilon^{2/3}k^{4/3} \tag{16}$$

$$\Pi_E^{\pm<} = \varepsilon^\pm - \frac{3}{4}C_E\nu\varepsilon^{2/3}k^{4/3} \tag{17}$$

$$\Pi_H^< = \delta - \frac{3}{2}C_H\nu\delta\varepsilon^{-1/3}k^{4/3} \tag{18}$$

$$\Pi_H^{\pm<} = \delta^\pm \mp \frac{3}{7}C_E\nu\varepsilon^{2/3}k^{7/3}. \tag{19}$$

From (16) to (19) we see that at zero order in k the fluxes are constant and equal to F_X^s, provided that F_X^s is not zero. The value $k = k_X^s$ for which $\Pi_X^{s<}(k) = 0$ is peculiar in the sense that for $k > k_X^s$ the dissipation of X^s is stronger than the injection rate F_X^s. We call it the dissipation scale of X^s. In the Kolmogorov theory the end of the (energy cascading) inertial range is given by the viscous scale

$$k_E = \left(\frac{2\varepsilon^{1/3}}{3C_E\nu}\right)^{3/4}. \tag{20}$$

For $k > k_E$ the viscous dissipation is dominant and (16) is not valid anymore.

The other scales for which $\Pi_X^{s<}(k) = 0$ are given by

$$k_H = (C_E/C_H)^{3/4}\, k_E \tag{21}$$

$$k_E^\pm = (2\varepsilon^\pm/\varepsilon)^{3/4}\, k_E \tag{22}$$

$$k_H^\pm/k_F = (7\varepsilon^\pm/2\varepsilon)^{3/7}(k_E/k_F)^{4/7} \tag{23}$$

In Ditlevsen & Giuliani (2001) the cancellation of the $k^{-5/3}$ terms in (10) and (11) has been ignored in the calculation of $H(k)$, leading to a different result for k_H. As in Chen *et al.* (2003) we predict that helicity H and energy E both dissipate at the viscous scale k_E, and that $H^\pm$ dissipates at a larger scale $k_H^\pm \propto k_E^{4/7}$. Taking $\nu = 10^{-7}$ and $\varepsilon = 1$ leads to $k_E \sim 10^5$. For $k_F \sim 1$ we further have $k_H^\pm \sim 10^3$. The difference between both scales k_E and $k_H^\pm$ should be visible in a shell model simulation, as shown in the next section.

3. Helical shell models for Navier-Stokes turbulence

Shell models of hydrodynamic turbulence originate back to the seventies with Lorenz (1972), Gledzer (1973) and Desnianskii & Novikov (1974). The main idea is to describe the statistics of homogeneous and isotropic turbulence in spectral space using a simple set of ordinary differential equations. The shells being logarithmically spaced, and taking one unknown per shell, such models allow to investigate some turbulence properties at a numerical cost drastically lower than a direct numerical simulation. It is then possible to reach Reynolds numbers defined at scale k_F by $Re = C_E^{1/2}\varepsilon^{1/3}k_F^{-4/3}\nu^{-1}$, as large as 10^7 as will be done below. Helical shell models were developed by Benzi *et al.* (1996), and are based on the helical Fourier modes decomposition as introduced above. As pointed out in Lessinnes *et al.* (2009), such helical modes can be retrieved from the helical triadic systems of the Navier-Stokes equations in helical basis. This approach leads to a single formula for four independent models:

$$d_t u_n^\pm = Q_n^\pm - \nu k_n^2 u_n^\pm + f_n^\pm, \tag{24}$$

with

$$\begin{aligned} Q_n^\pm &= ik_n\big[(s_1\lambda - s_2\lambda^2)u_{n+1}^{\pm s_1}u_{n+2}^{\pm s_2} \\ &+ (s_2\lambda - \lambda^{-1})\ u_{n-1}^{\pm\ s_1}u_{n+1}^{\pm s_2 s_1} \\ &+ (\lambda^{-2} - s_1\lambda^{-1})\ u_{n-2}^{\pm s_2}u_{n-1}^{\pm s_1 s_2}\big]^*, \end{aligned} \tag{25}$$

where each model is retrieved for one particular choice of (s_1, s_2) with $s_1,\ s_2 = \pm 1$. In (25) the parameter λ is the logarithmic shell spacing and the wave number is defined as $k_n = \lambda^n$. We use a forcing f_n only in the first shell ($k_F = 1$) with a random phase.

The shell model (25) is designed such that total energy E and helicity H are conserved in the absence of forcing and viscosity ν. They are defined by

$$E = \sum_{n=1}^{N} E_n, \qquad H = \sum_{n=1}^{N} H_n \tag{26}$$

where N is the number of shells in the model. The energy E_n and helicity H_n in shell n are defined in total analogy with equations (5) and (6)

$$E_n = E_n^+ + E_n^-, \quad E_n^\pm = \frac{1}{2}|u_n^\pm|^2, \tag{27}$$

$$H_n = H_n^+ + H_n^-, \quad H_n^\pm = \pm\frac{1}{2}k_n|u_n^\pm|^2 \tag{28}$$

The GOY model used in Ditlevsen & Giuliani (2001) corresponds taking $(s_1, s_2) = (-1, +1)$ in the helical model (25). In this case, two uncoupled sets of variables appear: $(u_1^+, u_2^-, u_3^+, \dots)$ and $(u_1^-, u_2^+, u_3^-, \dots)$. In the GOY model, only one of these sets is considered neglecting the other variables and thereby implying that only H_n^+ or H_n^- is described within each shell n but not both. Therefore the canceling of the leading terms in equations (10) and (11) leading to $H(k)$ in (8) can not be obtained with a GOY model. On the other hand, the arguments in Chen *et al.* (2003) where illustrated with the model corresponding to $(s_1, s_2) = (+1, -1)$. This time, all variables are coupled and both $H_n^\pm$ and H_n are available within each shell n. We shall prolongate this work in the rest of the paper investigating the energy and helicity spectra and fluxes in each helical mode or both.

For that we define the energy and helicity fluxes as

$$\Pi_E^<(n) = \Pi_E^{+<}(n) + \Pi_E^{-<}(n), \tag{29}$$

$$\Pi_H^<(n) = \Pi_H^{+<}(n) + \Pi_H^{-<}(n), \tag{30}$$

with

$$\Pi_E^{\pm<}(n) = -\sum_{m=1}^{n} Q_m^{\pm} u_m^{\pm *} + cc, \tag{31}$$

$$\Pi_H^{\pm<}(n) = \mp\sum_{m=1}^{n} k_m Q_m^{\pm} u_m^{\pm *} + cc. \tag{32}$$

These quantities are defined in total analogy with those of (14). In figures 1 and 2 the results are presented for respectively a helical and a non helical case. The parameters are $\nu = 10^{-7}$, $k_F = 1$ and $\lambda = 1.618$. For the helical case $\varepsilon^+ = \varepsilon = 1$, implying $\delta = \delta^+ = 1$ and $\varepsilon^- = \delta^- = 0$. For the non helical case $\varepsilon^+ = \varepsilon^- = 1/2$, implying $\varepsilon = 1$, $\delta^+ = -\delta^- = 0.5$ and $\delta = 0$. In each figure the top and bottom rows correspond respectively to energies and helicities.

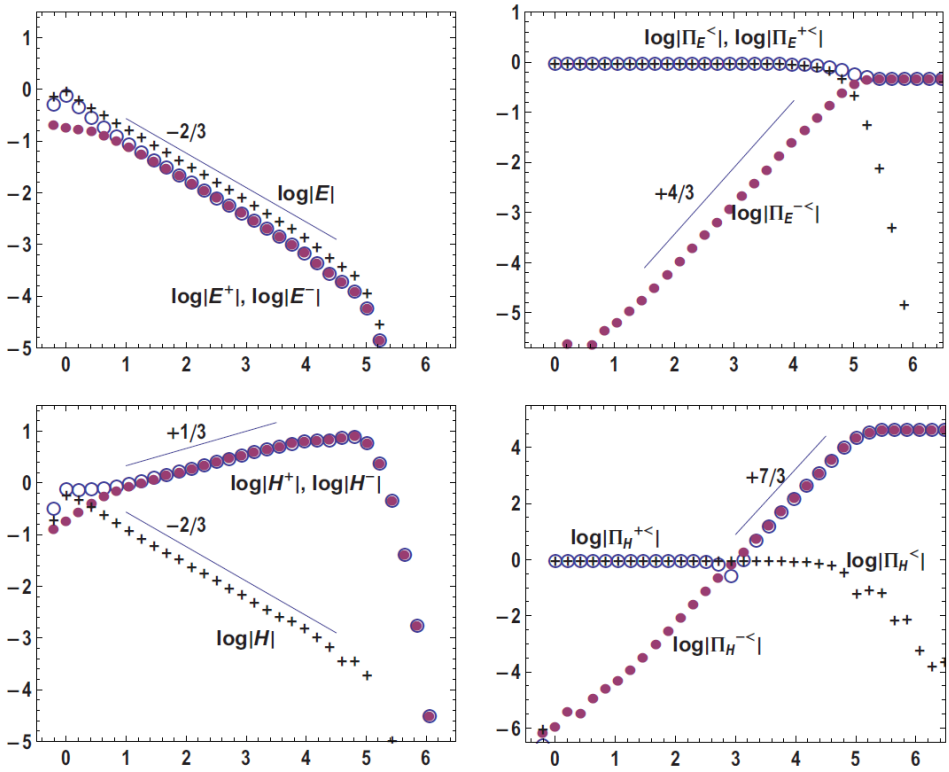

Figure 1. Helical case: $\varepsilon = \varepsilon^+ = 1$, $\delta^- = \varepsilon^- = 0$ ($\nu = 10^{-7}$). Energy and helicity are respectively represented on the top and bottom rows versus $\log k$.The positive and negative helical modes are denoted by ○ and ●, the sum of both modes by +.The spectra (resp. fluxes) are represented in the top (resp. down) row.

The spectra $\log_{10} X$ versus $\log_{10} k$ are plotted in the left column. Energies $E(k)$ and $E^{\pm}(k)$ scale in $k^{-2/3}$ (straight line) corresponding to power spectral densities in $k^{-5/3}$ in agreement with (4), (10) and (11). Helicities $H^{\pm}(k)$ scale in $k^{1/3}$ (straight line) corresponding to power spectral densities in $k^{-2/3}$ in agreement with (9). In the helical case, the total helicity $H(k)$ scales in $k^{-2/3}$ corresponding to a power spectral density in $k^{-5/3}$ in agreement with (4). In the non helical case $H(k)$ is the sum of two opposite quantities $H^{\pm}(k)$ and then has no clear scaling. Compared to $H^{\pm}(k)$ it can be considered as negligible, in agreement with (4) taking $\delta = 0$.

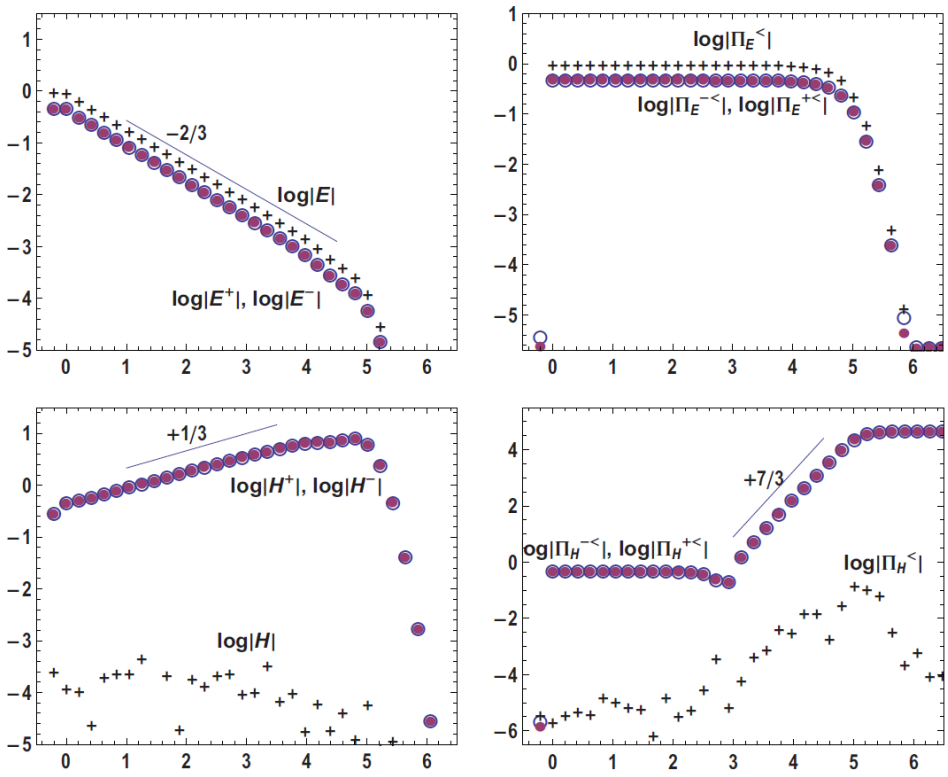

Figure 2. Non helical case: $\varepsilon^- = \varepsilon^+ = 1/2$, $\delta = 0$. The same presentation as in Fig. 1

In the right columns, fluxes are plotted in a $\log_{10}$-$\log_{10}$ frame. In the helical case we clearly see the power scalings expected from (17) and (19) in the inertial range. For such a helical case we have $\varepsilon^- = 0$ and $\delta^- = 0$ implying respectively $|\Pi_E^{-<}(k)| \propto k^{4/3}$ and $\Pi_H^{-<}(k) \propto k^{7/3}$. In addition we clearly identify the dissipation wave number $k_H^+ \sim 10^3$ such that for $k \geq k_H^+$ the dissipation of H^+ is larger than δ^+, implying from (19) that $|\Pi_H^{+<}(k)| \propto k^{7/3}$.

In the non helical case we also identify the dissipation wave numbers $k_H^+ = k_H^- \sim 10^3$ such that for $k \geq k_H^\pm$ the dissipation of $H^\pm$ is larger than $|\delta^\pm|$, implying from (19) that $|\Pi_H^{\pm<}(k)| \propto k^{7/3}$. The little overshoot at $k \sim 10^3$ is due to the absolute value representation of the sign change of $\Pi_H^{\pm<}(k)$.

4. Numerical aspects of the simulations

We summarize here four numerical issues that we had to face for our problem.

A first issue is related to the numerical stiffness of the system (25). Indeed from Navier-Stokes equations, or from (24), we can define two characteristic times $\tau_u \propto (ku)^{-1}$ and $\tau_\nu \propto (\nu k^2)^{-1}$ which are respectively the advective and diffusive time scales. The characteristic time of the problem corresponds to the smallest one between τ_u and τ_ν which is $\tau_u \propto (k)^{-2/3}$ in the inertial range, and $\tau_\nu \propto \nu^{-1}k^{-2}$ in the dissipative range. Therefore the characteristic time of the problem may vary considerably from large to small scales. In our simulations it is about unity for $k = 1$ and about 10^{-7} for $k = 10^7$ ($\nu = 10^{-7}$). To deal with this stiffness we use a VODE time-stepping scheme as suggested in Brown *et al.* (1998).

In addition, a high accuracy is needed here because we want to reproduce a helicity scaling $H(k) \propto k^{-5/3}$ resulting from the difference of the two terms $|H^+(k)|$ and $|H^-(k)|$, each one scaling as $|H^\pm(k)| \propto k^{-2/3}$ at leading order (see section 2). It corresponds to a ratio $|H(k)|/|H^\pm(k)| \propto k^{-1}$, which reaches a value as small as 10^{-5} for the parameters of figure 1 and 2. To reach this accuracy we take a relative error of 10^{-6} in the VODE time scheme.

An other source of error could arises if the dissipative range is not solved with a sufficiently large number of shells. Typically we take about 10 shells in the dissipative range, the energy of the 3 last ones remaining equal to zero.

Finally we have to deal with fluctuations of helicity $|H^\pm(k)|$ which are stronger than those of energy $|E^\pm(k)|$ by a factor k. Reaching statistically stationary spectra of helicity then requires more data. The convergence of the calculation versus the number of data is illustrated in figure 3. We find that increasing $\zeta = QT$, where Q is the number of independent runs each one performed during the same time T, the spectrum of H converges, in both cases helical and non helical. The convergence seems to scale as $\zeta^{-1/2}$. It is related to the formula

$$\delta\langle a\rangle = \frac{\delta a}{\sqrt{N}}, \tag{33}$$

where a is a Gaussian process, $\delta\langle a\rangle$ the variation of the mean value of a due to the finite sampling, δa the standard deviation of a and N the number of independent values of a within the sampling.

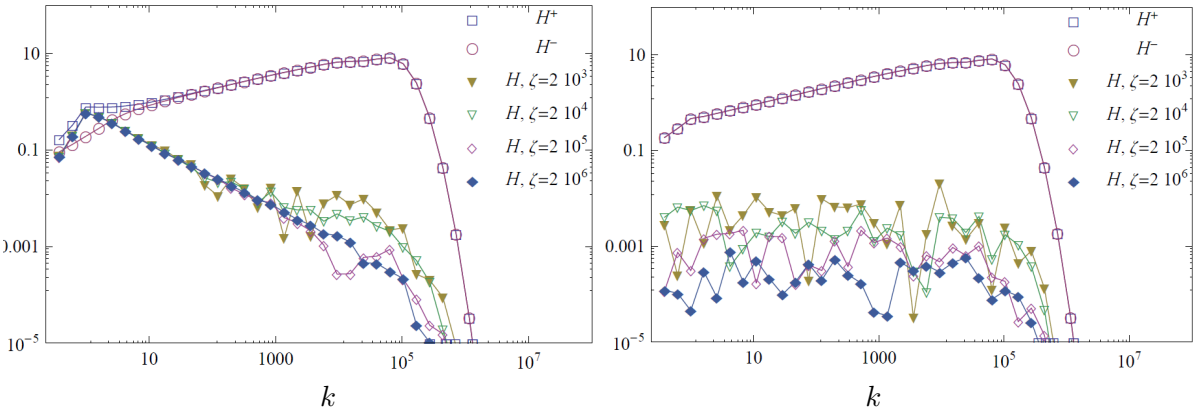

Figure 3. Mean helicity spectra for different amount of statistics measured by the parameter ζ, for the helical (left) and non helical (right) case.

References

Benzi, R., Biferale, L., Kerr, R. M. & Trovatore, E. 1996 Helical shell models for three-dimensional turbulence. *Physics Review E* **53**, 3541–3550.

Brown, P. N., Byrne, G. D. & Hindmarsh, A. C. 1998 VODE, a Variable-Coefficient ODE Solver. *SIAM. J. Sci. Stat. Comput.* **10**, 1038–1051.

Chen, Qiaoning, Chen, Shiyi & Eyink, Gregory L. 2003 The joint cascade of energy and helicity in three-dimensional turbulence. *Physics of Fluids* **15** (2), 361–374.

Desnianskii, V. N. & Novikov, E. A. 1974 Simulation of cascade processes in turbulent flows. *Prikladnaia Matematika i Mekhanika* **38**, 507–513.

Ditlevsen, P. D. & Giuliani, P. 2001 Cascades in helical turbulence. *Physics Review E* **63** (3), 036304.

Ditlevsen, P. D. & Giuliani, P. 2001 Dissipation in helical turbulence. *Physics of Fluids* **13** (11), 3508–3509.

Gledzer, E. B. 1973 System of hydrodynamic type admitting two quadratic integrals of motion. *Soviet Physics Doklady* **18**, 216–+.

Lessinnes, T., Plunian, F. & Carati, D. 2009 Helical shell models for MHD. *Theoretical and Computational Fluid Dynamics* **23**, 439–450.

Lessinnes, T., Plunian, F., Stepanov, R. & Carati, D. 2011 Dissipation scales of kinetic helicities in turbulence. *Physics of Fluids* **23** (3), 035108.

Lorenz, E. N. 1972 Low order models representing realizations of turbulence. *Journal of Fluid Mechanics* **55**, 545–563.

Waleffe, Fabian 1992 The nature of triad interactions in homogeneous turbulence. *Physics of Fluids A: Fluid Dynamics* **4** (2), 350–363.